



PERGAMON

Available online at [www.sciencedirect.com](http://www.sciencedirect.com)

SCIENCE @ DIRECT®

International Journal of Non-Linear Mechanics 39 (2004) 281–297

INTERNATIONAL JOURNAL OF

**NON-LINEAR  
MECHANICS**

[www.elsevier.com/locate/nlm](http://www.elsevier.com/locate/nlm)

# Staggering error control of a class of inelastic processes in random microheterogeneous solids

T.I. Zohdi\*

*Department of Mechanical Engineering, 6195 Etcheverry Hall, University of California, Berkeley, CA 94720-1740, USA*

## Abstract

In this work a staggering solution strategy for the simulation of the time-dependent inelastic mechanical deformation of a class of solids, possessing irregular heterogeneous microstructure, is developed. The system of coupled equations involved consists of (1) a dynamic equation of momentum balance, where the primary field variable is the displacement, (2) an evolution equation for material degradation, where the primary field variable is a state damage function, and (3) an evolution equation for the inelastic strains in the solid where the primary field variable is a plastic strain field. Clearly, the damage and plasticity variables are implicit functions of the displacement, however, for the staggering scheme strategy, it is convenient to formulate them as individual fields during the solution process. The key concept for the strategy to operate efficiently is to estimate and control the so-called staggering error, i.e. the error due to incompletely resolving the coupling between the field equations in a staggering process. This error is a function of the time step size. However, because the coupling is temporally variable, possibly becoming stronger, weaker, or oscillatory, it is extremely difficult to ascertain a priori the time step size needed for prespecified error control. In the present work, to induce desired staggering rates of convergence within each time step, thus controlling the staggering error, an adaptive strategy is developed whereby the time step size is manipulated, enlarged or reduced, to control the intrinsic contraction mapping constant of the staggering system operator. The overall goal is to deliver accurate solutions where temporal discretization error control dictates the upper limits on the time step size, while the iterative staggering strategy refines the step size further to control the staggering error. Three-dimensional numerical experiments are performed to illustrate the solution strategy.  
© 2003 Elsevier Science Ltd. All rights reserved.

*Keywords:* Multiphase materials; Coupled inelastic fields; Staggering error

## 1. Introduction

One reason for the success of many modern structural components is the *tailored* macroscopic behavior of the material, which can be achieved by modifying a homogeneous base matrix material's behavior by adding second-phase microscale particulates. However, a drawback of adding particulate material to a homogeneous base matrix is that the presence of second phase particles will perturb the otherwise smooth stress fields in the matrix, locally amplifying or reducing the fields throughout the microstructure, which in turn can lead to inhomogeneous damage and plastic growth throughout the microstructure of the

\* Tel.: +1-510-642-9172; fax: +1-510-642-6163.

E-mail address: [zohdi@newton.berkeley.edu](mailto:zohdi@newton.berkeley.edu) (T.I. Zohdi).

material. In the ideal case, one would like to make predictions, via numerical simulations, of whether adding a certain type of matrix-particulate combination will have poor inelastic behavior to minimize expensive laboratory tests. The focus of this work is primarily on the numerical and algorithmic aspects of the solution to a class of time-dependent deformation processes involving simultaneous damage and plasticity in solids possessing randomly distributed particulate microstructure. The model considered is based on a somewhat standard time-dependent overstress formulation that closely resembles models found in Huet [1–3], Huet et al. [4] and Huet [5–8]. A nonlinearly coupled partial differential equation system arises. Schemes based on attempts to solve the entire system simultaneously (monolithically), then applying Newton-type algorithms, are not robust due to the possibility of zero, or near zero, tangents that occur when describing a weakening material.<sup>1</sup> As an example, consider a material law of the form  $\sigma = \alpha \mathbb{E}_0 : \varepsilon$ , where  $\mathbb{E}_0$  is the virgin undamaged material, and  $\alpha$  is the classical continuity (isotropic damage) parameter introduced by Kachanov [9], where  $\alpha(t=0) = 1$  indicates an initial state, where  $0 < \alpha \leq 1$  and  $\dot{\alpha} \leq 0$ . The scalar function  $\alpha$  takes on different values throughout the body, dictated by the evolution law. This constitutive law possesses a tangent of the form  $d\sigma = d\alpha \mathbb{E}_0 : \varepsilon + \alpha \mathbb{E}_0 : d\varepsilon \stackrel{\text{def}}{=} \mathbb{E}^{\text{TAN}} : d\varepsilon$ . In this case,  $\mathbb{E}^{\text{TAN}}$  can lose positive definiteness when the change in  $\alpha$  is sufficiently large, which in turn will lead to an indefinite system of algebraic equations. This is one primary reason why explicit-type schemes enjoy wide usage for complicated phenomena involving damage.

One can interpret solution techniques of so-called “staggering-type” used in multifield simulation processes, whereby, within a time step, each field equation or evolution law is solved individually, allowing only the primary field variable to be active, as a type of explicit approach, *if the process is not recursive within a time step*. In explicit staggering schemes, after the solution of each field equation, the primary field variable is updated, and the next field equation is addressed in a similar manner. In the standard approach, after this process has been applied, only once, to all of the field equations, the time step is incremented and the procedure is repeated. The classical solution process is nonrecursive, and is highly sensitive to the order in which the staggered field equations are solved. The order of staggering is usually selected based upon somewhat ad hoc arguments pertaining to which field “drives” the other. *When there is complicated coupling, it is extremely difficult to ascertain in what order to stagger the solution process*. Furthermore, as time progresses, for complicated systems, the coupling can change, becoming stronger, weaker or oscillatory. For accurate numerical solutions, explicit approaches require small time steps, primarily because the staggering error accumulates with each passing increment. For details, see Park and Felippa [10], Zienkiewicz [11], Schrefler [12], Lewis et al. [13] and Doltsinis [14]. A particularly lucid review can be found in Lewis and Schrefler [15].

In this work a solution strategy for the simulation of the time-dependent inelastic mechanical deformation of a class of solids, possessing irregular heterogeneous microstructure, is developed. The system of equations involved are (1) an equation of momentum balance, where the primary field variable is the displacement, (2) an evolution equation for material degradation, where the primary field variable is a damage state function, and (3) an evolution equation for the inelastic strains in the solid where the primary field variable is a plastic strain field. Clearly, the damage and plasticity variables are implicitly functions of the displacement, however, for the staggering scheme strategy, it is convenient to formulate them as individual fields during the solution process. For this class of problems, in order to accurately capture the microstructure, it is inescapable that one must use extremely fine finite element meshes, and thus the resulting system of algebraic equations to be solved can be quite large. The key concept for the strategy to operate efficiently is to estimate and control the so-called staggering error, i.e. the error due to incompletely resolving the coupling between the field equations in a staggering process. This error is a function of the time step size. However, because

<sup>1</sup> Clearly, for homogeneous materials exhibiting rate independent plasticity in the absence of damage, a Newton scheme, for example based on the concept of consistent linearization is preferable.

the coupling is temporally variable, possibly becoming stronger, weaker, or oscillatory, it is extremely difficult to ascertain a priori the time step size needed for prespecified error control. In the present work, a solution strategy is developed, whereby the time step size is manipulated, enlarged or reduced, to control the intrinsic contraction mapping constant of system staggering operator in order to induce desired staggering rates of convergence within each time step, thus controlling the staggering error. The approach builds on a technique developed in Zohdi [16]. The overall goal is to deliver accurate solutions where the minimum of the time step needed for temporal discretization error control and the time step needed for staggering error control,  $\Delta t_{\text{tol}} = \min(\Delta t^{\text{discrete}}, \Delta t^{\text{Staggering}})$ , dictates the upper limits on the time step size. Numerical experiments are performed to illustrate the solution strategy in practical three-dimensional settings involving solids possessing irregular heterogeneous microstructure.

The outline of the presentation is as follows. In Section 2, a model problem is developed to describe the deformation of a heterogeneous solid at finite strains. In Section 3, a recursive, temporally adaptive, fixed-point type staggering solution scheme, based on *spectral-radius/contraction-constant* control is developed. The approach is based on the observation that the iterative rates of convergence are inversely proportional to the time step size. Therefore, if the iterative process converges too slowly, then the time step size is appropriately reduced to increase the convergence rates. Conversely, the step sizes are enlarged, reducing the computational effort, when the staggering convergence rates exceed the prescribed limit. In either case, within a time step, the staggering rates of convergence, and the staggering error, are controlled, essentially by manipulating the iterative contraction mapping constant of the fixed point system. In Section 4, numerical experiments are given to illustrate the solution strategy in a practical three-dimensional setting for materially and geometrically nonlinear systems. In Section 5, some concluding comments are given.

## 2. A model problem

A structure which occupies an open bounded domain in  $\Omega \in \mathbb{R}^3$ , with boundary  $\partial\Omega$ , is considered. The boundary consists of  $\Gamma_u$  on which the displacements ( $\mathbf{u}$ ) are prescribed and a part  $\Gamma_t$  on which tractions are prescribed. The mechanical properties of the heterogeneous material are characterized by a spatially varying elasticity tensor  $\mathbb{E} \in \mathbb{R}^{3^2 \times 3^2}$  and various evolution (rate) parameters for describing inelastic strains and damage in the material.  $\mathbb{E}$  is assumed to be a symmetric bounded positive definite tensor-valued function. For reasons of clarity, strong forms are used to derive the governing equations, possibly assuming more regularity than warranted. Afterwards, only the weak forms, which produce solutions that coincide with those of strong formulations, when the solutions are smooth enough, are employed.

### 2.1. Constitutive assumptions: infinitesimal strain case

We first discuss infinitesimal strains and then a finite strain analog. To a first approximation the constitutive relationship can be written as  $\boldsymbol{\sigma} = \mathbb{E} : (\boldsymbol{\varepsilon} - \boldsymbol{\beta})$ , where  $\boldsymbol{\sigma}$  is the Cauchy stress. The symbol  $\boldsymbol{\beta}$  is used for the inelastic strains. Specifically, we describe the material changes (damage) and plastic strains via evolution laws of the following form:<sup>2</sup>

$$\boldsymbol{\sigma} = \underbrace{\alpha \mathbb{E}_0}_{\mathbb{E}} : (\boldsymbol{\varepsilon} - \boldsymbol{\beta}), \quad \boldsymbol{\beta} = \boldsymbol{\varepsilon}_\lambda,$$

<sup>2</sup> The field  $\boldsymbol{\beta}$  could, in general, include other effects, such as thermal strains.

$$\dot{\alpha} = \underbrace{\left( a_1 \left( \frac{\|\boldsymbol{\sigma}'\|}{\|\boldsymbol{\sigma}'_{\text{crit}}\|} - 1 \right) + a_2 \left( \frac{|\text{tr } \boldsymbol{\sigma}/3|}{|\text{tr } \boldsymbol{\sigma}/3|_{\text{crit}}} - 1 \right) \right)}_{g_\alpha} \alpha \quad (0 < \alpha \leq 1),$$

$$\dot{\lambda} = \underbrace{\left( a_3 \left( \frac{\|\boldsymbol{\sigma}'\|}{\|\boldsymbol{\sigma}'_{\text{crit}}\|} - 1 \right) \right)}_{g_\lambda} \lambda \Rightarrow \boldsymbol{\varepsilon}_\lambda \stackrel{\text{def}}{=} \dot{\lambda} \mathbf{h} \Rightarrow \boldsymbol{\varepsilon}_\lambda = \int_0^t \dot{\lambda} \mathbf{h} dt \quad \left( \mathbf{h} \stackrel{\text{def}}{=} \frac{\boldsymbol{\sigma}'}{\|\boldsymbol{\sigma}'\|} \right), \tag{2.1}$$

with the following activation conditions:

- if  $\|\boldsymbol{\sigma}'\| \stackrel{\text{def}}{=}} \sqrt{\boldsymbol{\sigma}' : \boldsymbol{\sigma}'} < \boldsymbol{\sigma}'_{\text{crit}}$  then  $a_1 = a_3 = 0$ ,
- if  $\|\boldsymbol{\sigma}'\| \stackrel{\text{def}}{=}} \sqrt{\boldsymbol{\sigma}' : \boldsymbol{\sigma}'} \geq \boldsymbol{\sigma}'_{\text{crit}}$  then  $a_1 = a_1^* < 0$ ,  $a_3 = a_3^* > 0$ ,
- if  $|\frac{\text{tr } \boldsymbol{\sigma}}{3}| < |\frac{\text{tr } \boldsymbol{\sigma}}{3}|_{\text{crit}}$  then  $a_2 = 0$  and
- if  $|\frac{\text{tr } \boldsymbol{\sigma}}{3}| \geq |\frac{\text{tr } \boldsymbol{\sigma}}{3}|_{\text{crit}}$  then  $a_2 = a_2^* < 0$ .

Here  $a_1^*$ ,  $a_2^*$  and  $a_3^*$ ,  $\boldsymbol{\sigma}'_{\text{crit}} \stackrel{\text{def}}{=} k_1(\boldsymbol{\sigma}'/\|\boldsymbol{\sigma}'\|)$ ,  $\text{tr } \boldsymbol{\sigma}_{\text{crit}}/3 \stackrel{\text{def}}{=} k_2$ ,  $k_1$  and  $k_2$  are spatially variable material parameters,  $\boldsymbol{\sigma}' = \boldsymbol{\sigma} - (\text{tr } \boldsymbol{\sigma}/3)\mathbf{1}$  and where  $\boldsymbol{\varepsilon}_\lambda$  represents plastic strains. As indicated in the introduction, here  $\mathbb{E} = \alpha \mathbb{E}_0$ , where  $\mathbb{E}_0$  is the virgin undamaged material, and  $\alpha$  is the classical continuity (isotropic damage) parameter (Kachanov [9]), where  $\alpha(t = 0) = 1$  indicates an initial state. The scalar function  $\alpha$  takes on different values throughout the body, as dictated by the evolution law. For any later time  $t$ , one can consider a deteriorating (weakening) material where  $0 < \alpha \leq 1$  ( $a_1$  and  $a_3$  being negative), and where as  $\alpha \rightarrow 0$  the material becomes completely damaged. For further details on these types of phenomenological (damage) formulations, the interested reader is referred to the classical work of Kachanov [9].

### 2.2. A geometrically-nonlinear extension

Now we construct a geometrically nonlinear formulation, as an extension to the infinitesimal strain case. We consider the case of finite deformations with small elastic strains ( $\leq \approx 1\%$ ) and moderate inelastic strains. Later in the work, an updated Lagrangian staggering type scheme, formulated directly in the current configuration, will be used, and thus current configuration-based material laws are advantageous. A relatively straightforward extension to the infinitesimal deformation constitutive laws is to employ the Eulerian/Almansi strain tensor<sup>3</sup> ( $\mathbf{L} \stackrel{\text{def}}{=} \frac{1}{2}(\mathbf{1} - \mathbf{b}^{-1}) = \frac{1}{2}(\nabla_x \mathbf{u} + (\nabla_x \mathbf{u})^T - (\nabla_x \mathbf{u})^T \cdot \nabla_x \mathbf{u})$ :

$$\boldsymbol{\sigma} = \underbrace{\alpha \mathbb{E}_0}_{\mathbb{E}} : (\mathbf{L} - \boldsymbol{\beta}), \quad (\boldsymbol{\beta} = \mathbf{L}_\lambda),$$

$$\dot{\alpha} = \underbrace{\left( a_1 \left( \frac{\|\boldsymbol{\sigma}'\|}{\|\boldsymbol{\sigma}'_{\text{crit}}\|} - 1 \right) + a_2 \left( \frac{|\text{tr } \boldsymbol{\sigma}/3|}{|\text{tr } \boldsymbol{\sigma}/3|_{\text{crit}}} - 1 \right) \right)}_{g_\alpha} \alpha \quad (0 < \alpha \leq 1),$$

$$\dot{\lambda} = \underbrace{\left( a_3 \left( \frac{\|\mathbf{S}'\|}{\|\mathbf{S}'_{\text{crit}}\|} - 1 \right) \right)}_{g_\lambda} \lambda \Rightarrow \mathbf{L}_\lambda = \mathbf{F} \cdot \left( \int_0^t \dot{\lambda} \mathbf{h} dt \right) \cdot \mathbf{F}^T \quad \left( \mathbf{h} \stackrel{\text{def}}{=} \frac{\mathbf{S}'}{\|\mathbf{S}'\|} \right), \tag{2.2}$$

where  $\mathbf{b} = \mathbf{F} \cdot \mathbf{F}^T$ ,  $\mathbf{F} = \nabla_X \mathbf{x}$ ,  $\boldsymbol{\sigma}'_{\text{crit}} \stackrel{\text{def}}{=} k_1(\boldsymbol{\sigma}'/\|\boldsymbol{\sigma}'\|)$ ,  $(\text{tr } \boldsymbol{\sigma}_{\text{crit}}/3) \stackrel{\text{def}}{=} k_2$ ,  $k_1$  and  $k_2$  being material constants,  $\boldsymbol{\sigma}' = \boldsymbol{\sigma} - (\text{tr } \boldsymbol{\sigma}/3)\mathbf{1}$ ,  $\mathbf{S}' = \mathbf{J}\mathbf{F}^{-1} \cdot \boldsymbol{\sigma}' \cdot \mathbf{F}^{-T}$ ,  $\mathbf{S}'_{\text{crit}} = \mathbf{J}\mathbf{F}^{-1} \cdot \boldsymbol{\sigma}'_{\text{crit}} \cdot \mathbf{F}^{-T}$  with flow activation conditions specified as specified

<sup>3</sup> As in the infinitesimal strain case, the field  $\boldsymbol{\beta}$  could include other effects, such as thermal strains.

previously where  $\mathbf{u}=\mathbf{x}-\mathbf{X}$ ,  $\mathbf{X}$  are referential coordinates and in the isotropic case  $\mathbf{x}$  are current coordinates. The symbol  $\nabla_{\mathbf{x}}$  indicates differentiation with respect to the current configuration. Such a law is frame indifferent under rigid body rotations and translations. Clearly,  $\mathbf{L}$  is objective as are the scalar-based evolution laws for  $\alpha$  and  $\lambda$ . By construction, the geometrically nonlinear formulation matches the geometrically linear case for infinitesimal deformations. In the context of plasticity, if one adheres to the split  $\mathbf{F} = \mathbf{F}_e \cdot \mathbf{F}_p$ , then  $\mathbf{E} - \mathbf{E}_p = \frac{1}{2} \mathbf{F}_p^T \cdot (\mathbf{F}_e^T \cdot \mathbf{F}_e - \mathbf{1}) \cdot \mathbf{F}_p$ , where  $\mathbf{E} = \frac{1}{2} (\mathbf{F}^T \cdot \mathbf{F} - \mathbf{1})$ . The Eulerian split is closely related to the well-known split of Green and Naghdi [17–19],  $\mathbf{E}_e \stackrel{\text{def}}{=} \mathbf{E} - \mathbf{E}_p$ , where  $\mathbf{E}$ ,  $\mathbf{E}_e$  and  $\mathbf{E}_p$  are the total, “elastic” and plastic Green–Lagrange strains, has been used. Casey [19] justifies the Green–Naghdi split as an approximation valid for small elastic and moderate plastic strains. Computational aspects of such strain splits, in the context of pure elastoplasticity, are discussed in Simo and Ortiz [20] and Simo [21]. We remark that  $\mathbf{E}_e$  is not a true elastic strain, except in very special cases. One can simply consider  $\mathbf{E} - \mathbf{E}_p$  as an internal parameter used in a constitutive law, which is not intended to have any kinematical meaning at finite strains. The Eulerian type of split is merely a “push forward” of  $\mathbf{E} - \mathbf{E}_p$ . We remark that the coefficients  $a_1$  through  $a_3$  could be temperature dependent, although in this work we do not consider this case. Also, we remark that for the plastic strain, the manipulations involving the Second Piola–Kirchhoff stress,  $\mathbf{S}$ , are necessary to achieve a frame-indifferent constitutive formulation. For the damage this is unnecessary due to the fact that it is a purely scalar quantity. It is important to note that the constitutive law relating the Cauchy stress and the Almansi strain tensor must be isotropic in order to remain frame indifferent under all superposed rigid body rotations. To see this consider,  $[\hat{\boldsymbol{\sigma}}] = [\mathbf{R}][\boldsymbol{\sigma}][\mathbf{R}]^T$  implying  $\{\hat{\boldsymbol{\sigma}}\} = [\mathbf{T}]\{\boldsymbol{\sigma}\} = [\hat{\mathbf{E}}][\mathbf{T}]\{\mathbf{L}\} = [\hat{\mathbf{E}}]\{\hat{\mathbf{L}}\}$  which implies  $\{\boldsymbol{\sigma}\} = [\mathbf{T}^{-1}][\hat{\mathbf{E}}][\mathbf{T}]\{\mathbf{L}\}$ , where  $[\mathbf{R}]$  is a transformation matrix, and where  $[\cdot]$  is used to indicate matrix notation equivalent to a tensor form, while  $\{\cdot\}$  is used to indicate a vector representation. Frame indifference requires that  $[\mathbf{E}] = [\mathbf{T}^{-1}][\hat{\mathbf{E}}][\mathbf{T}]$ ,  $\forall [\mathbf{R}]$  and thus  $\forall [\mathbf{T}]$ . This relation holds only if  $[\mathbf{E}]$  is isotropic.

### 3. A recursive staggering algorithm

As indicated in the introduction, a popular class of solution techniques for coupled systems are so-called “staggering schemes”, whereby, within a time step, each field equation is solved individually, allowing only the primary field variable to be active. After the solution of each field equation, the primary field variable is updated, and the next field equation is addressed in a similar manner. In an explicit variant of such an approach, after this process has been applied, only once, to all of the field equations, the time step is incremented and the procedure is repeated. An explicit type of this process is nonrecursive, and for accurate numerical solutions, the approach requires small time steps, primarily because the staggering error accumulates with each passing increment. For details, see Park and Felippa [10], Zienkiewicz [11], Schrefler [12], Lewis et al. [13], Doltsinis [14], Piperno [22], Lewis and Schrefler [15] and Le Tallec and Mouro [23]. In Zohdi [5], a recursive staggering strategy which allowed the adaptive control of time step sizes, was developed. In that approach, in order to reduce the error within a time step, the staggering methodology was formulated as a recursive fixed-point iteration, whereby the system was repeatedly re-solved until fixed-point type convergence was achieved. Extending the approach in Zohdi [16] to the class of problems at hand, we consider a system consisting of four fields:  $\mathbf{u}$ ,  $\theta$ ,  $\alpha$  and  $\mathbf{L}_\lambda$ . Clearly, the *pseudo-field* variables,  $\alpha$  and  $\mathbf{L}_\lambda$ , are implicitly functions of the displacement, i.e.  $\alpha = \alpha(\mathbf{u})$  and  $\mathbf{L}_\lambda = \mathbf{L}_\lambda(\mathbf{u})$ , however, for the staggering scheme strategy, it is convenient to formulate them as individual fields. In some cases, inertial terms can play an important role in the model under consideration. A relatively straightforward approach for the inertial terms, which is amenable to time step adaptivity, is ( $L$  being the time step counter)

$$\ddot{\mathbf{u}}^{L+1} = \frac{\dot{\mathbf{u}}^{L+1} - \dot{\mathbf{u}}^L}{\Delta t} = \frac{(\mathbf{u}^{L+1} - \mathbf{u}^L)/\Delta t - \dot{\mathbf{u}}^L}{\Delta t} = \frac{\mathbf{u}^{L+1} - \mathbf{u}^L}{(\Delta t)^2} - \frac{\dot{\mathbf{u}}^L}{\Delta t} = \frac{\mathbf{u}^{L+1}}{(\Delta t)^2} - \frac{\mathbf{u}^L}{(\Delta t)^2} - \frac{\dot{\mathbf{u}}^L}{\Delta t}, \quad (3.1)$$

which collapses to a central difference-like stencil of  $\ddot{\mathbf{u}}^{L+1} = (\mathbf{u}^{L+1} - 2\mathbf{u}^L + \mathbf{u}^{L-1})/(\Delta t)^2$ , when the time step size is uniform. For the evolution equations, consistent with the fully staggered solution approach we freeze the  $g_x$  and  $g_\lambda$ , using the most current state variable values, and integrate analytically. *Additionally, the geometric configuration of the system is frozen during each equation solve, and is updated only at the end of each individual system iteration.* This is essentially an “updated Lagrangian” formulation, where all variables are referred to the last calculated configuration as opposed to a “total Lagrangian” formulation where all variables are referred to the initial configuration. In this particular case, the last calculated configuration is the previously computed one within the staggering scheme. Employing weak formulations, algorithmically the staggering scheme is as follows:

AT A TIME STEP (L) : START AN INTERNAL ITERATION I = 0

STEP 1 : UPDATE GEOMETRICAL CONFIGURATION :  $\Omega^{L+1,I} = \Omega^{L+1,I-1}$

STEP 2 : INTEGRATE EVOLUTION EQUATIONS

$$\dot{\alpha}^{L+1,I+1} = g_x^{L+1,I} \alpha^{L+1,I+1} \Rightarrow \alpha^{L+1,I+1} = \alpha^L e^{g_x^{L+1,I} \Delta t^{L+1}},$$

$$\dot{\lambda}^{L+1,I+1} = g_\lambda^{L+1,I+1/2} \lambda^{L+1,I+1} \Rightarrow \lambda^{L+1,I+1} = \lambda^L e^{g_\lambda^{L+1,I} 1/2 \Delta t^{L+1}}$$

WHERE  $g^{L+1,I} \stackrel{\text{def}}{=} g(\mathbf{u}^{L+1,I} \alpha^{L+1,I+1})$

STEP 3 : SOLVE BALANCE OF MOMENTUM :

Find  $\mathbf{u}^{L+1,I+1} \in U_u(\Omega^{L+1,I})$ ,  $\mathbf{u}^{L+1,I+1}|_{\Gamma_u^{L+1,I}} = \mathbf{d}^{L+1}$  such that  $\forall \mathbf{v} \in V_u(\Omega^{L+1,I})$ ,  $\mathbf{v}|_{\Gamma_u^{L+1,I}} = \mathbf{0}$

$$\begin{aligned} & \int_{\Omega^{L+1,I}} \nabla_x \mathbf{v} : \alpha^{L+1,I} \left( \mathbb{E}_0 : (\nabla_x \mathbf{u}^{L+1,I+1} - \frac{1}{2} (\nabla_x \mathbf{u}^{L+1,I})^T \cdot \nabla_x \mathbf{u}^{L+1,I} - \boldsymbol{\beta}^{L+1,I+1}) \right) d\Omega \\ & + \int_{\Omega^{L+1,I}} \rho^{L+1,I} \frac{\mathbf{u}^{L+1,I+1}}{(\Delta t)^2} \cdot \mathbf{v} d\Omega - \int_{\Omega^{L+1,I}} \rho^{L+1,I} \left( \frac{\mathbf{u}^L}{(\Delta t)^2} + \frac{\dot{\mathbf{u}}^L}{\Delta t} \right) \cdot \mathbf{v} d\Omega \\ & - \int_{\Omega^{L+1,I}} \mathbf{f}^{L+1,I} \cdot \mathbf{v} d\Omega - \int_{\Gamma_t^{L+1,I}} \mathbf{t}^{L+1,I} \cdot \mathbf{v} dA = 0 \end{aligned} \quad (3.2)$$

WHERE :  $\boldsymbol{\beta}^{L+1,I+1} \stackrel{\text{def}}{=} \mathbf{L}_\lambda^{L+1,I+1}$

STEP 4 : CHECK FOR CONVERGENCE :  $\frac{\|\mathbf{u}^{L+1,I+1} - \mathbf{u}^{L+1,I}\|_{L^1(\Omega^{L+1,I})}}{\|\mathbf{u}^{L+1,I+1}\|_{L^1(\Omega^{L+1,I})}} \leq \text{TOL}$

STEP 5 : IF TOLERANCE NOT MET THEN  $I = I + 1$ , GO TO STEP 1,

STEP 6 : IF TOLERANCE MET THEN INCREMENT TIME :  $L = L + 1$ , UPDATE ALL VARIABLES.

Here  $U_u$  is the space of admissible trial functions, while  $V_u$  is the space of admissible test functions. For most loading cases and data these spaces will correspond to  $\mathbf{H}^1$ . In an abstract setting, one can consider the following active set solution strategy where the underlined variable is momentarily active, the corresponding field equations solved, the active variable updated, and the process repeated for the next field equation:

$$\begin{aligned} \mathcal{A}_1(\alpha^{I+1}, \underline{\mathbf{L}}_\lambda^I, \mathbf{u}^I) &= \mathcal{F}_2(\alpha^I, \mathbf{L}_\lambda^I, \mathbf{u}^I), \dots, \text{etc.} \quad (\text{DEGRADATION}), \\ \mathcal{A}_2(\alpha^{I+1}, \underline{\mathbf{L}}_\lambda^{I+1}, \mathbf{u}^I) &= \mathcal{F}_2(\alpha^{I+1}, \mathbf{L}_\lambda^I, \mathbf{u}^I), \dots, \text{etc.} \quad (\text{PLASTICITY}), \\ \mathcal{A}_3(\alpha^{I+1}, \mathbf{L}_\lambda^{I+1}, \underline{\mathbf{u}}^{I+1}) &= \mathcal{F}_3(\alpha^{I+1}, \mathbf{L}_\lambda^{I+1}, \mathbf{u}^I), \dots, \text{etc.} \quad (\text{MOMENTUM}). \end{aligned} \quad (3.3)$$

Writing the system in the form presented leads to algebraic systems which are symmetric and positive definite. Therefore, standard iterative solvers such as the preconditioned Conjugate Gradient Method, can be used. Such solvers are highly advantageous since any previous solution, from a previous time step or staggered iteration can be used as the first guess in the solution procedure, thus providing a “head start” in the solution process.

#### 4. Issues of convergence and staggering error control

The algorithm outlined in Boxes 3.2 and 3.3 can be considered as a fixed-point scheme, whose convergence within each time step is dependent on the time step size itself. The step size can be manipulated, enlarged or reduced, to induce the desired rates of convergence within a time step, in order to achieve an error tolerance within a prespecified number of iterations. Consider the general equation

$$A(\mathbf{w}) = \mathbf{F}. \tag{4.1}$$

It is advantageous to write this in the form

$$\mathbf{\Pi}(\mathbf{w}) = A(\mathbf{w}) - \mathbf{F} = \mathbf{G}(\mathbf{w}) - \mathbf{w} + \mathbf{r} = \mathbf{0}. \tag{4.2}$$

A straightforward fixed point iterative scheme is

$$\mathbf{G}(\mathbf{w}^{I-1}) + \mathbf{r} = \mathbf{w}^I \tag{4.3}$$

The convergence of such a scheme is dependent on the behavior of  $\mathbf{G}$ . Namely, a sufficient condition for convergence is that  $\mathbf{G}$  be a contraction mapping for all  $\mathbf{w}^I$ ,  $I = 1, 2, 3 \dots$ . Convergence of the iteration can be studied by defining the error vector  $\mathbf{e}^I = \mathbf{w}^I - \mathbf{w}$ . A necessary condition for convergence is iterative self-consistency, i.e. the exact solution must be represented by the scheme  $\mathbf{G}(\mathbf{w}) + \mathbf{r} = \mathbf{w}$ . Enforcing this condition, a sufficient condition for convergence is the existence of a contraction mapping

$$\|\mathbf{e}^I\| = \|\mathbf{w}^I - \mathbf{w}\| = \|\mathbf{G}(\mathbf{w}^{I-1}) - \mathbf{G}(\mathbf{w})\| \leq \eta \|\mathbf{w}^{I-1} - \mathbf{w}\|, \tag{4.4}$$

where, if  $\eta < 1$  for each iteration  $I$ , then  $\mathbf{e}^I \rightarrow \mathbf{0}$  for any arbitrary starting solution  $\mathbf{w}^{I=0}$  as  $I \rightarrow \infty$ . If  $\mathbf{G}$  is differentiable, we may write

$$\mathbf{G}(\mathbf{w}) = \mathbf{G}(\mathbf{w}^{I-1}) + \nabla_{\mathbf{w}} \mathbf{G}(\mathbf{w})|_{\mathbf{w}^{I-1}} (\mathbf{w}^I - \mathbf{w}^{I-1}) + \mathcal{O}(\|\Delta \mathbf{w}\|^2), \tag{4.5}$$

and thus, provided that the functional behavior is locally convex (Perron [24], Ostrowski [25,26], Ortega and Rockoff [27] and Kitchen [28]) in the neighborhood of the solution,

$$\begin{aligned} \|\mathbf{G}(\mathbf{w}) - \mathbf{G}(\mathbf{w}^{I-1})\| &= \|\nabla_{\mathbf{w}} \mathbf{G}(\mathbf{w})|_{\mathbf{w}^{I-1}} (\mathbf{w}^I - \mathbf{w}^{I-1}) + \mathcal{O}(\|\Delta \mathbf{w}\|^2)\| \\ &\leq \|\nabla_{\mathbf{w}} \mathbf{G}(\mathbf{w})|_{\mathbf{w}^{I-1}} (\mathbf{w}^I - \mathbf{w}^{I-1})\| \quad (\text{local convexity}) \\ &\leq \underbrace{\|\nabla_{\mathbf{w}} \mathbf{G}(\mathbf{w})|_{\mathbf{w}^{I-1}}\|}_{\eta^{I-1}} \|\mathbf{w}^I - \mathbf{w}^{I-1}\|. \end{aligned} \tag{4.6}$$

Therefore, unconditional convergence is attained if for  $\mathbf{w}^I$ ,  $I = 1, 2, 3, \dots$ ,  $\eta^I < 1$ . General overviews of fixed-point algorithms can be found in Ames [29].

**Remark.** An alternative approach is to attempt to solve the entire system simultaneously (monolithically). This would involve the use of a Newton-type scheme, which can also be considered as a type of fixed-point iteration. Newton’s method is covered as a special case of this general analysis. To see this, consider  $\mathbf{\Pi}(\mathbf{w}^I) = \mathbf{\Pi}(\mathbf{w}^{I-1}) + \nabla_{\mathbf{w}} \mathbf{\Pi}_{\mathbf{w}^{I-1}}(\mathbf{w}^I - \mathbf{w}^{I-1}) + \mathcal{O}(\|\Delta \mathbf{w}\|^2) \approx 0$ . Therefore, Newton updating can be written as

$$\mathbf{w}^I = \mathbf{w}^{I-1} - (\mathbf{A}^{\text{TAN},I-1})^{-1} \mathbf{\Pi}(\mathbf{w}^{I-1}), \tag{4.7}$$

where  $\mathbf{\Pi} \stackrel{\text{def}}{=} \mathbf{A}(\mathbf{w}) - \mathbf{F}$  is the residual, and  $\mathbf{A}^{\text{TAN},I} = (\nabla_{\mathbf{w}} \mathbf{A}(\mathbf{w}))|_{\mathbf{w}^I} = (\nabla_{\mathbf{w}} \mathbf{\Pi}(\mathbf{w}))|_{\mathbf{w}^I}$  is the tangent. Therefore, in the fixed-point form one has the operator  $\mathbf{G}(\mathbf{w}) = \mathbf{w} - (\mathbf{A}^{\text{TAN}})^{-1} \mathbf{\Pi}(\mathbf{w})$ . The gradient is  $\nabla_{\mathbf{w}} \mathbf{G}(\mathbf{w}) = (\mathbf{A}^{\text{TAN}})^{-2} (\mathbf{A}^{\text{TAN}})^{\text{TAN}} \mathbf{\Pi}(\mathbf{w})$ , where  $(\mathbf{A}^{\text{TAN}})^{\text{TAN}} \stackrel{\text{def}}{=} \nabla_{\mathbf{w}} (\nabla_{\mathbf{w}} \mathbf{A}(\mathbf{w}))$ . Therefore, the convergence criterion is,  $\forall I = 1, 2, \dots$ , following the approach for the first fixed-point scheme,

$$\|\mathbf{G}(\mathbf{w}) - \mathbf{G}(\mathbf{w}^{I-1})\| \leq \underbrace{\|(\mathbf{A}^{\text{TAN},I-1})^{-2} (\mathbf{A}^{\text{TAN},I-1})^{\text{TAN},I-1} \mathbf{\Pi}(\mathbf{w}^{I-1})\|}_{\eta^{I-1}} \|\mathbf{w}^{I-1} - \mathbf{w}\|. \tag{4.8}$$

Equivalently, one can write  $\|((\nabla_{\mathbf{w}} \mathbf{\Pi})^{-2} \nabla_{\mathbf{w}} (\nabla_{\mathbf{w}} \mathbf{\Pi}(\mathbf{\Pi}(\mathbf{w}))))|_{\mathbf{w}^{I-1}}\| < 1$ . As mentioned at the outset of this work, one immediately sees a fundamental difficulty, due to the possibility of a zero, or near zero, tangent when employing a Newton-type method to a system describing a weakening material, since  $\mathbb{E}^{\text{TAN}}$  can lose positive definiteness when the change in  $\alpha$  is sufficiently large, which in turn will lead to an indefinite-type system of algebraic equations. Therefore, while Newton’s method usually converges at a faster rate than a direct fixed point iteration, quadratic as opposed to superlinear, its convergence behavior is less robust than the presented fixed-point algorithm, due to its dependence on the gradients of the solution. In this work, since we consider materials which experience damage and plasticity, under dynamic conditions, it is unlikely that the gradients of  $\mathbf{G}$  remain positive definite and thus we opt for the more robust “gradient-free” staggering scheme. A further issue complicating the use of Newton-type schemes for simulating microheterogeneous solids is the low regularity of the operator  $\mathbf{G}$  with respect to  $\mathbf{w}$ , thus making gradients highly unattractive and in many cases inapplicable.

#### 4.1. Explicit time dependence

For the class of coupled systems considered in this work the coupled operator’s spectral radius is directly dependent on the time step discretization  $\Delta t$ . We consider a simple example which illustrates the essential concepts. Consider coupling of a second-order system and two first-order systems

$$\begin{aligned} a\dot{w}_1 + w_2 &= 0, \\ b\dot{w}_2 + w_3 &= 0, \\ c\ddot{w}_3 + w_1 &= 0. \end{aligned} \tag{4.9}$$

When discretized in time, for example with a backward Euler scheme,  $\dot{w}_1^{L+1} = (w_1^{L+1} - w_1^L) / \Delta t$ ,  $\dot{w}_2^{L+1} = (w_2^{L+1} - w_2^L) / \Delta t$  and  $\ddot{w}_3^{L+1} = (w_3^{L+1} - 2w_3^L + w_3^{L-1}) / (\Delta t)^2$ , one obtains the following coupled system:

$$\begin{bmatrix} 1 & \frac{\Delta t}{a} & 0 \\ 0 & 1 & \frac{\Delta t}{b} \\ \frac{(\Delta t)^2}{c} & 0 & 1 \end{bmatrix} \begin{Bmatrix} w_1^{L+1} \\ w_2^{L+1} \\ w_3^{L+1} \end{Bmatrix} = \begin{Bmatrix} w_1^L \\ w_2^L \\ 2w_3^L - w_3^{L-1} \end{Bmatrix}, \tag{4.10}$$

where  $L$  is a time increment counter. For a recursive staggering scheme of Jacobi-type, where the updates are made only after one complete iteration, considered here only for algebraic simplicity, one has<sup>4</sup>

$$\begin{bmatrix} 1 & 0 & 0 \\ 0 & 1 & 0 \\ 0 & 0 & 1 \end{bmatrix} \begin{Bmatrix} w_1^{L+1,I+1} \\ w_2^{L+1,I+1} \\ w_3^{L+1,I+1} \end{Bmatrix} = \begin{Bmatrix} w_1^L \\ w_2^L \\ 2w_3^L - w_3^{L-1} \end{Bmatrix} - \begin{Bmatrix} \frac{\Delta t}{a} w_1^{L+1,I} \\ \frac{\Delta t}{b} w_2^{L+1,I} \\ \frac{(\Delta t)^2}{c} w_3^{L+1,I} \end{Bmatrix}. \tag{4.11}$$

Rewriting this in terms of the  $\mathbf{G}$ -form yields

$$\underbrace{\begin{bmatrix} 0 & \frac{\Delta t}{a} & 0 \\ 0 & 0 & \frac{\Delta t}{b} \\ \frac{(\Delta t)^2}{c} & 0 & 0 \end{bmatrix}}_{\mathbf{G}} \begin{Bmatrix} w_1^{L+1,I} \\ w_2^{L+1,I} \\ w_3^{L+1,I} \end{Bmatrix} - \underbrace{\begin{Bmatrix} w_1^L \\ w_2^L \\ 2w_3^L - w_3^{L-1} \end{Bmatrix}}_r - \underbrace{\begin{Bmatrix} w_1^{L+1,I+1} \\ w_2^{L+1,I+1} \\ w_3^{L+1,I+1} \end{Bmatrix}}_{w^{L+1,I+1}}. \tag{4.12}$$

The eigenvalues of  $\mathbf{G}$  are  $\pm(\Delta t)^{4/3}/(abc)^{1/3}$ . One sees that the spectral radius of the staggering operator grows quasilinearly with the time step size, specifically, superlinearly as  $(\Delta t)^{4/3}$ . Following Zohdi [16], a somewhat less algebraically complicated example illustrates a further characteristic of such solution processes. Consider the following example of reduced dimensionality, namely a coupled first-order system  $aw_1 + w_2 = 0$  and  $bw_2 + w_1 = 0$ . When discretized in time with a backward Euler scheme and repeating the preceding procedure one obtains the following  $\mathbf{G}$ -form:

$$\underbrace{\begin{bmatrix} 0 & \frac{\Delta t}{a} \\ \frac{\Delta t}{b} & 0 \end{bmatrix}}_{\mathbf{G}} \begin{Bmatrix} w_1^{L+1,I} \\ w_2^{L+1,I} \end{Bmatrix} - \underbrace{\begin{Bmatrix} w_1^L \\ w_2^L \end{Bmatrix}}_r - \underbrace{\begin{Bmatrix} w_1^{L+1,I+1} \\ w_2^{L+1,I+1} \end{Bmatrix}}_{w^{L+1,I+1}}. \tag{4.13}$$

The eigenvalues of  $\mathbf{G}$  are  $\pm\sqrt{(\Delta t)^2/ab}$ . One sees that the convergence of the staggering scheme is directly related (linearly in this case) to the size of the time step. The solution to the example is

$$w_1^{L+1} = \frac{abw_1^L + b\Delta tw_2^L}{ab - (\Delta t)^2} = \underbrace{w_1^L - \frac{w_2^L}{a} \Delta t}_{\text{first staggered iteration}} + \underbrace{\frac{w_1^L}{ab} (\Delta t)^2}_{\text{second staggered iteration}} + \dots \tag{4.14}$$

and

$$w_2^{L+1} = \frac{abw_2^L + a\Delta tw_1^L}{ab - (\Delta t)^2} = \underbrace{w_2^L - \frac{w_1^L}{a} \Delta t}_{\text{first staggered iteration}} + \underbrace{\frac{w_2^L}{ab} (\Delta t)^2}_{\text{second staggered iteration}} + \dots \tag{4.15}$$

As pointed out in Zohdi [16], the time step induced restriction for convergence matches the radius of analyticity of a Taylor series expansion of the solution, which converges in a ball of radius from the point of expansion

---

<sup>4</sup> A Gauss–Seidel-type approach would involve using the most current iterate. Typically, under very general conditions, if the Jacobi method converges, the Gauss–Seidel method converges at a faster rate, while if the Jacobi method diverges, the Gauss–Seidel method diverges at a faster rate. The Jacobi method is easier to address theoretically, thus it is used for proof of convergence, and the Gauss–Seidel method at the implementation level.

to the nearest singularity, around the previous time increment solution. In other words, the limiting step size is given by setting the denominator to zero,  $ab - (\Delta t)^2 = 0$ , which is in agreement with the condition derived from the analysis of the eigenvalues of  $\mathbf{G}$ .

Generally speaking, if the recursive process is *not employed*, i.e. an explicit scheme, the staggering error can accumulate relatively rapidly. However, an overkill approach involving very small time steps, smaller than needed to control the discretization error, simply to suppress a nonrecursive staggering process error, is computationally inefficient. Therefore, the objective of the next section is to develop a strategy to adaptively adjust, in fact maximize, the choice of the time step size to control the staggering error, while simultaneously staying below a critical time step size needed to control the discretization error. An important related issue is to simultaneously minimize the computational effort involved. The number of times the multifield system is solved, as opposed to time steps, is taken as the measure of computational effort, since within a time step, many multifield system re-solves can take place.

#### 4.2. Contraction-mapping time stepping control

The type of contraction condition discussed is sufficient, but not necessary, for convergence. In order to construct an adaptive staggering strategy, we modify an approach in Zohdi [16] originally developed for thermochemical multifield problems, one approximates  $\eta \approx S(\Delta t)^p$ , where one estimates the error within an iteration to behave according to  $(S(\Delta t)^p)^I e^0 = e^I$ ,  $I = 1, 2, \dots$ , where  $e^0$  is the initial staggering error and  $S$  is a function intrinsic to the system. *Our target or ideal condition is to meet an error tolerance in a given number of iterations, not more, and not less.* One writes this in the following approximate form,  $(S(\Delta t_{\text{tol}})^p)^{I_d} e^0 = \text{TOL}$ , where  $I_d$  is the number of desired iterations. Therefore, if the error tolerance is not met in a desired number of iterations, the contraction constant  $\eta$  is too large. Accordingly, one can solve for a new smaller step size, under the assumption that  $S$  is constant,

$$\Delta t_{\text{tol}} = \Delta t \left( \frac{(\text{TOL}/e^0)^{1/pI_d}}{(e^I/e^0)^{1/pI}} \right). \quad (4.16)$$

The assumption that  $S$  is constant is not overly severe, since the time steps are to be recursively refined and unrefined. Clearly, the expression in Eq. (4.16) is used for time step enlargement, if convergence is met in less than  $I_d$  iterations. One sees that if  $e^{I_d} > e_{\text{tol}}$  and  $I = I_d$ , then the expression in Eq. (4.16) collapses to a ratio of the error tolerance to the achieved level of iterative error after  $I_d$  iterations,  $\Delta t_{\text{tol}} = \Delta t (\text{TOL}/e^{I_d})^{1/pI_d}$ , and thus the step size will be scaled by the ratio of the error to the tolerance. We first define the normalized error, within each time step ( $L + 1$ )

$$e^{I \text{ def}} \equiv \frac{\|\mathbf{u}^{L+1,I} - \mathbf{u}^{L+1,I-1}\|_{L^1(\Omega)}}{\|\mathbf{u}^{L+1,I}\|_{L^1(\Omega)}} \quad (4.17)$$

and its corresponding violation ratio

$$\psi^{I \text{ def}} \equiv \frac{e^I}{\text{TOL}}. \quad (4.18)$$

Here, a general formulation has been written for a more general set of variables, which will be introduced later. One then determines the violation  $\psi^I$  and a scaling factor

$$\phi^{I \text{ def}} \equiv \left( \frac{(\text{TOL}/e^0)^{1/pI_d}}{(e^I/e^0)^{1/pI}} \right). \quad (4.19)$$

Thereafter, the following criterion for temporal adaptivity is adopted

IF TOLERANCE MET ( $\psi^I \leq 1$ ) AND  $I < I_d$  THEN :

(a) CONSTRUCT NEW TIME STEP  $\Delta t = \phi^I \Delta t$  AND  $t = t + \Delta t$

(b) SELECT MINIMUM :  $\Delta t = \text{MIN}(\Delta t^{\text{discrete}}, \Delta t)$

(c) STEP TIME :  $t = t + \Delta t$  AND START AT TIME STEP  $(L + 1)$

IF TOLERANCE NOT MET ( $\psi^I > 1$ ) AND  $I \geq I_d$  THEN : (4.20)

(a) STEP BACK :  $t = t - \Delta t$

(b) CONSTRUCT NEW TIME STEP :  $\Delta t = \phi^{I_d} \Delta t$

(c) SELECT MINIMUM :  $\Delta t = \text{MIN}(\Delta t^{\text{discrete}}, \Delta t)$

(d) RESTART AT TIME STEP  $L + 1$

### 5. Numerical experiments

To illustrate the algorithm, we considered a cube of matrix material, with normalized dimensions  $1 \times 1 \times 1$ , containing randomly distributed inhomogeneities. The various physical properties of the two materials are shown in Table 1. We consider a set of topological microstructural variables which can be conveniently parametrized by a generalized “ellipsoid”

$$\left(\frac{|x - x_o|}{r_1}\right)^{s_1} + \left(\frac{|y - y_o|}{r_2}\right)^{s_2} + \left(\frac{|z - z_o|}{r_3}\right)^{s_3} = 1, \tag{5.1}$$

where the  $s$ 's are exponents. Values of  $s < 1$  produce nonconvex shapes, while  $s > 2$  values produce “block-like” shapes. The types of suspensions to be introduced in the matrix binder can be controlled by (1) the polynomial order,  $s_1$ ,  $s_2$  and  $s_3$ , (2) the aspect ratios defined by  $\text{AR} \stackrel{\text{def}}{=} r_1/r_2 = r_1/r_3$ , where  $r_2 = r_3$ ,  $\text{AR} > 1$  for prolate geometries and  $\text{AR} < 1$  for oblate shapes and (3) the volume fractions. We considered the following boundary conditions on the exterior of the cube:  $\mathbf{u}(t=0)|_{\partial\Omega} = \mathbf{0}$ ,  $\mathbf{u}(t)|_{\partial\Omega} = t \times \mathcal{E} \cdot \mathbf{X}$ ,  $\mathcal{E}_{ij} = 0.01$ ,  $i, j = 1, 2, 3$ , where  $\mathbf{X}$  is a referential position vector to the boundary of the cube. We note that while the displacement loading is relatively small, the internal strains may be significantly larger. The material parameters, *selected only for the purposes of numerical experiment*, are shown in Table 1. From a practical engineering point of view,

Table 1  
Material properties used in the computational examples

Material property	Matrix	Particles
$\kappa$ (GPa)	78	230
$\mu$ (GPa)	26	172
$a_1^*$ ( $\frac{1}{\text{sec}}$ )	-0.1, -0.05, -0.01	-0.2, -0.1, -0.02
$a_2^*$ ( $\frac{1}{\text{sec}}$ )	-0.1, -0.05, -0.01	-0.2, -0.1, -0.02
$a_3^*$ ( $\frac{1}{\text{sec}}$ )	0.0001, 0.00005, 0.00001	0.00005, 0.000025, 0.00005
$k_1$ (MPa)	100	300
$k_2$ (MPa)	100	300
$\rho$ (kg/m <sup>3</sup> )	2700	2330

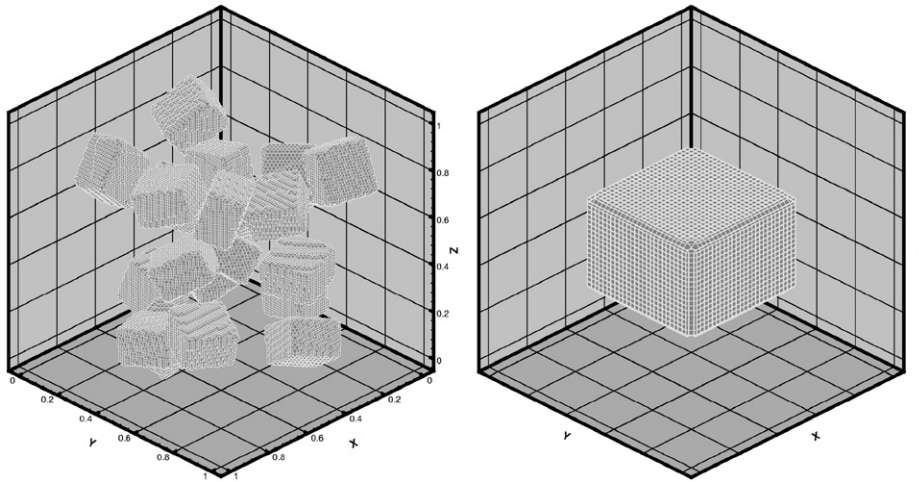


Fig. 1. Left: The numerical resolution of  $s = 10$  particles, with an (oblate) aspect ratio of  $r_1 = 0.7r_2 = 0.7r_3$ , resulting in a volume fraction of  $v_2 \approx 0.135$  (20 particles shown). Right: A single particle.

macroscopic quantities, which are volumetrically averaged outcomes of the simulated microstructural events, are of interest. Such quantities include, (1) the mechanical response,  $\langle \sigma \rangle_\Omega$  and (2) the average change in the material, for example damage,  $\langle \alpha \rangle_\Omega$ . For any microstructural combination, volume fractions, phase contrasts, etc., the samples must be tested and enlarged, holding the volume fraction constant, but increasing the number of particles, for example from 2, 4, ... until the macroscopic results stabilize. Over the course of such tests the finite element meshes were repeatedly refined, and a mesh density of approximately  $9 \times 9 \times 9$  trilinear hexahedra (approximately between 2200 and 3000 DOF for the vector-valued balance of momentum) *per particle* was found to deliver mesh independent results. Therefore, for example for the 10 particle test, 24000 DOF for the balance of momentum equation, for 20 particles, 46875 DOF, etc. During the computations, a “ $\frac{2}{5}$ ” Gauss rule was used, whereby elements containing material discontinuities had increased Gauss rules ( $5 \times 5 \times 5$ ) to enhance the resolution of the internal geometry, while elements with no material discontinuities had the nominal  $2 \times 2 \times 2$  rule. The numerical resolution of the microstructure is shown in Fig. 1, for a topological exponent of  $s = 10$ . Samples containing approximately 20 particles were used, although strictly speaking they were far too small to be statistically representative. However, they gave reasonably stable macroscopic results for the purposes of these numerical experiments. A more detailed and rigorous analysis of size effects for such systems is beyond the scope of this presentation. The reader is referred to the following series of works Huet [30–34], Guidoum and Navi [36], Amieur et al. [37], Guidoum [38], Amieur [39], Hazanov and Huet [40], Hazanov and Amieur [41], Amieur et al. [42] and Huet [6–8], as well as some recent work of the author (Zohdi [16,43]). In particular, for related work in the optimization of the material microstructure, controlling parameters such as  $s$ , see Zohdi [43].

A time step size of one second was the starting value. The algorithmic staggering tolerance was set to  $e \leq 0.0001$  for the normalized/global control. The designated maximum number of internal iterations,  $I_d$ , was set to five. However, during the simulations, this level of coarse time step discretization was not encountered. The starting time step size was  $\Delta t = 1$  s. In order to smoothly refine and unrefine the time steps, the time step contractions and enlargements were bounded in the range  $0.9 \leq \phi^I \leq 1.1$ . The total simulation time was set to 60 s. The time step limit size was set to 1 s. This was done in order to illustrate that the approach can be used when there is a maximum step size limit, for example set for reasons of time discretization (truncation) error control. No lower time step size was set. The results are depicted in Figs. 2–7 for strong,

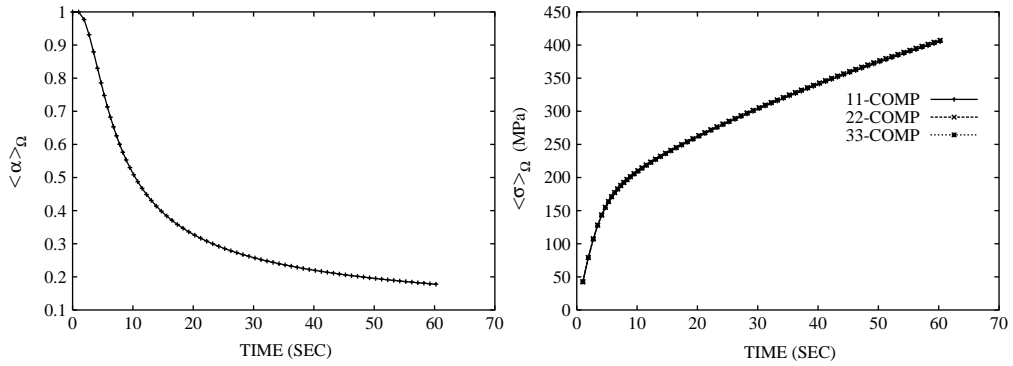


Fig. 2. For the *strongest* damage and plasticity rates (Table 1). Left: The volumetric average of the degradation versus time. Right: The volumetric average of the normal stresses versus time.

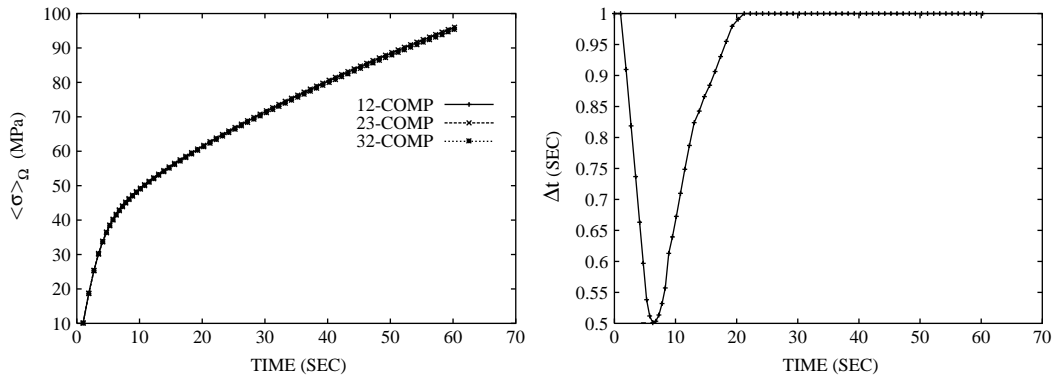


Fig. 3. For the *strongest* damage and plasticity rates (Table 1). Left: The volumetric average of the shear stresses versus time. Right: The adapted time step sizes versus time.

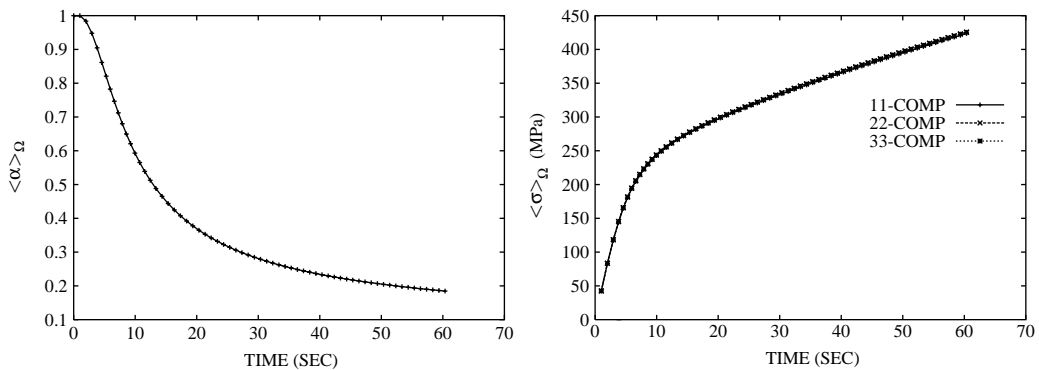


Fig. 4. For the *moderate* damage and plasticity rates (Table 1). Left: The volumetric average of the degradation versus time. Right: The volumetric average of the normal stresses versus time.

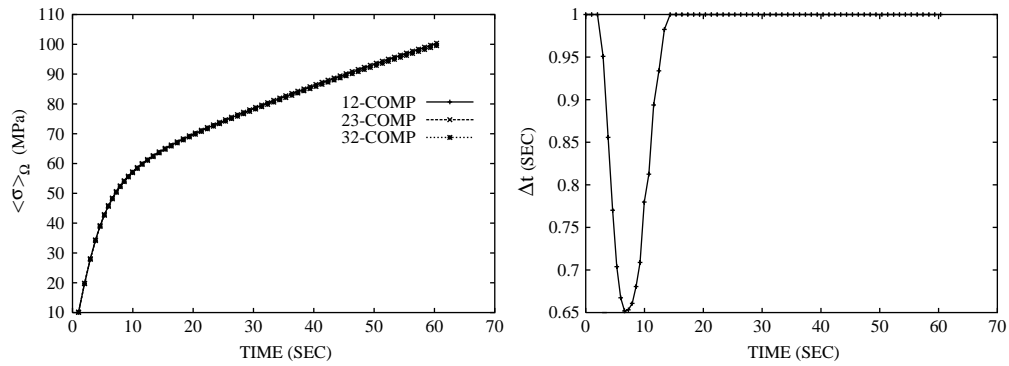


Fig. 5. For the moderate damage and plasticity rates (Table 1). Left: The volumetric average of the shear stresses versus time. Right: The adapted time step sizes versus time.

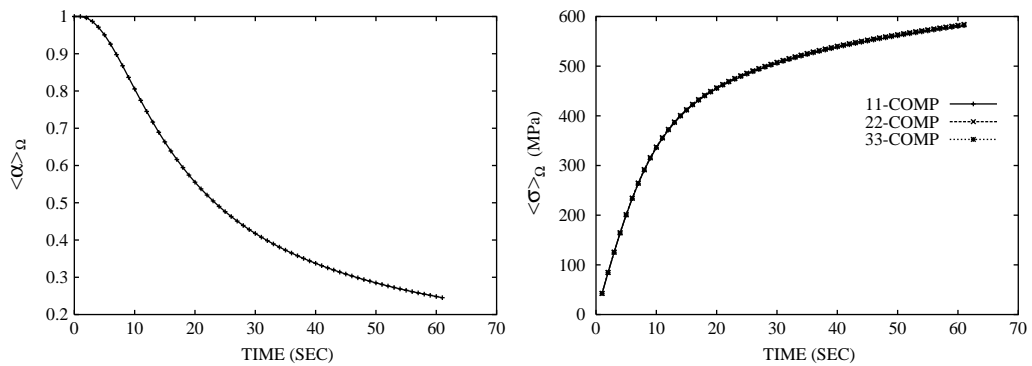


Fig. 6. For the weakest damage and plasticity rates (Table 1). Left: The volumetric average of the degradation versus time. Right: The volumetric average of the normal stresses versus time.

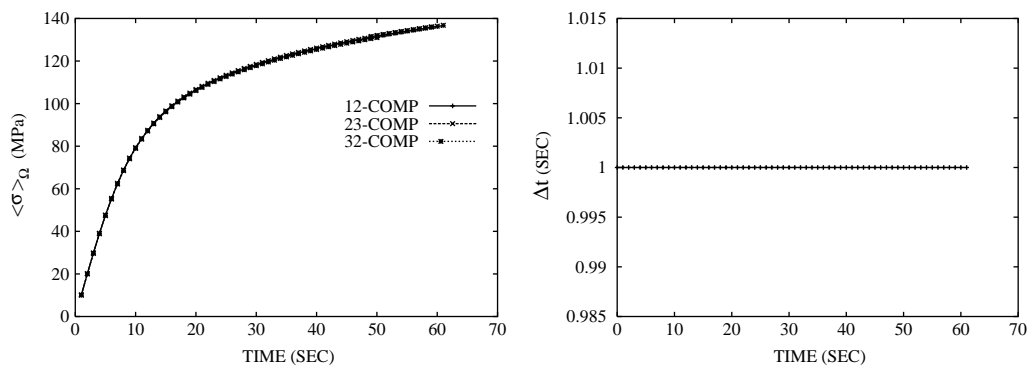


Fig. 7. For the weakest damage and plasticity rates (Table 1). Left: The volumetric average of the shear stresses versus time. Right: The time step sizes versus time (no adaptation was necessary).

moderate and weak damage and plasticity rates (Table 1). As the figures indicate, initially the time step size needed for the coupling error control was larger than that needed for the discretization error control. For the weakest damage and plasticity rates (Figs. 6–7), the time discretization error step size limit was adequate to control the staggering error as well. However, when significant inelastic effects become stronger (Figs. 2–5), the time steps required for staggering error control are smaller than those needed for time step discretization error control.

## 6. Concluding remarks

In this work, the error due to incompletely resolving the coupling between field equations describing time-dependent damage and plasticity in solids possessing irregular microstructure was characterized in such a way to be amenable to relatively simple adaptive control. A solution strategy was developed, whereby the time step size was manipulated, enlarged or reduced, to control the contraction mapping constant of the system operator in order to induce desired staggering rates of convergence within each time step. The overall goal was to deliver accurate solutions where the staggering error was controlled while simultaneously obeying time-step size limits dictated by discretization error concerns. Generally speaking, the error, which is a function of the time step size, is temporally variable and can become stronger, weaker, or possibly oscillatory, is extremely difficult to ascertain a priori as a function of the time step size. Therefore, to circumvent this problem, the adaptive strategy presented in this work was developed to provide accurate solutions by adjusting the time steps accordingly. Specifically, a sufficient condition for the convergence of the presented fixed-point scheme was that the spectral radius or contraction constant of the coupled operator, which depends on the time step size, must be less than unity. This observation was used to adaptively maximize the time step sizes, while simultaneously controlling the coupled operator's spectral radius, in order to deliver solutions below an error tolerance within a prespecified number of desired iterations. This recursive staggering error control can allow for substantial reduction of computational effort by the adaptive use of large time steps. Furthermore, such a recursive process has a reduced sensitivity, relative to an explicit approach, to the order in which the individual equations are solved, since it is self-correcting.

## References

- [1] C. Huet, Thermo-hygro-mechanical couplings in wood technology and rheological behaviours, in: H.D. Bui, Q.S. Nguyen (Eds.), *Thermomechanical Couplings in Solids*, IUTAM Symposium, Paris, 1986, North-Holland, Amsterdam, 1987, pp. 163–182.
- [2] C. Huet, Modeling the kinetics of the thermo-hygro-viscoelastic behavior of wood under constant climatic conditions, in: R. Itani (Ed.), *Proceedings of the 1988 International Conference on Timber Engineering*, Seattle, 1988, pp. 395–401.
- [3] C. Huet, Hybrid continuum thermodynamics framework and numerical simulations examples for the delayed micromechanical behavior of heterogeneous materials with chemical, climatic and defect sensitivity, in: Q.S. Nguyen, V.D. Nguyen (Eds.), *Engineering Mechanics Today*, Proceedings of the International Conference, Hanoi, University of Hanoi, pp. 170–184.
- [4] C. Huet, A. Guidoum, P. Navi, A 3D micromechanical model for numerical analysis and prediction of long term deterioration in concrete, in: K. Sakai, N. Banthia, O.E. Gjorv (Eds.), *Concrete under Severe Conditions: Environment and Loading*, Vol. 2, Spon, London, 1995, pp. 1458–1467.
- [5] C. Huet, Recent advances in the long term deformation and deterioration behavior of structural materials and components through the integrated micromechanics and thermodynamics of solids approach, in: A. Gerdes (Ed.), *Advances in Building Materials*, Aedificatio, Freiburg, 1996, pp. 161–196.
- [6] C. Huet, Activities 1989–1996, in: P. Navi, A. Tolou (Eds.), *Laboratory for Building Materials*, Department of Materials Report, 1997.
- [7] C. Huet, An integrated micromechanics and statistical continuum thermodynamics approach for studying the fracture behaviour of microcracked heterogeneous materials with delayed response, *Eng. Fracture Mech.* 58 (5–6) (1997) 459–556 (Special Issue).

- [8] C. Huet, Coupled size and boundary condition effects in viscoelastic heterogeneous bodies, *Mech. Mater.* 31 (12) (1999) 787–829.
- [9] L.M. Kachanov, *Introduction to Continuum Damage Mechanics*, Martinus Nijhoff, Dordrecht, 1986.
- [10] K.C. Park, C.A. Felippa, Partitioned analysis of coupled systems. in: T. Belytschko, T.J.R. Hughes (Eds.), *Computational Methods for Transient Analysis*, 1983. North-Holland Pub. Co. pp. 157–219.
- [11] O.C. Zienkiewicz, Coupled problems and their numerical solution, in: R.W. Lewis, P. Bettes, E. Hinton (Eds.), *Numerical Methods in Coupled Systems*, Wiley, Chichester, 1984, pp. 35–58.
- [12] B.A. Schrefler, A partitioned solution procedure for geothermal reservoir analysis, *Comm. Appl. Numer. Meth.* 1 (1985) 53–56.
- [13] R.W. Lewis, B.A. Schrefler, L. Simoni, Coupling versus uncoupling in soil consolidation, *Internat. J. Numer. Anal. Meth. Geomech.* 15 (1992) 533–548.
- [14] I.St. Doltsinis, Coupled field problems—solution techniques for sequential and parallel processing, in: M. Papadrakakis (Ed.), *Solving Large-Scale Problems in Mechanics*.
- [15] R.W. Lewis, B.A. Schrefler, *The Finite Element Method in the Static and Dynamic Deformation and Consolidation of Porous Media*, 2nd Edition, Wiley Press, New York, 1997.
- [16] T.I. Zohdi, An adaptive-recursive staggering strategy for simulating multifield coupled processes in microheterogeneous solids, *Internat. J. Numer. Methods Eng.* 53 (2002) 1511–1532.
- [17] A.E. Green, P.M. Naghdi, A general theory of an elasto-plastic continuum, *Arch. Rat. Mech. Anal.* 18 (1965) 251–281.
- [18] A.E. Green, P.M. Naghdi, Some remarks on elastoplastic deformation at finite strain, *Internat. J. Eng. Sci.* 9 (1971) 1219–1229.
- [19] J. Casey, Approximate kinematical relations in plasticity, *Internat. J. Solids Structures* 21 (1985) 671–682.
- [20] J.C. Simo, M. Ortiz, A unified approach to finite deformation elastoplastic analysis based on the use of hyperelastic constitutive laws, *Comput. Methods Appl. Mech. Eng.* 49 (1985) 221–245.
- [21] J.C. Simo, A framework for finite strain elastoplasticity based on maximum plastic dissipation and the multiplicative decomposition: part I. Continuum formulation, *Comput. Meth. Appl. Mech. Eng.* 66 (1988) 199–219.
- [22] S. Piperno, Explicit/implicit fluid/structure staggered procedures with a structural predictor and fluid subcycling for 2D inviscid aeroelastic simulations, *Internat. J. Numer. Meth. Fluids.* 25 (1997) 1207–1226.
- [23] P. Le Tallec, J. Mouro, Fluid structure interaction with large structural displacements, *Comput. Meth. Appl. Mech. Eng.* 190 (24–25) (2001) 3039–3067.
- [24] O. Perron, Über Stabilität und asymptotisches Verhalten der Lösungen eines Systems endlicher Differenzgleichungen, *J. Reine Angew. Math.* 161 (1929) 41–64.
- [25] A. Ostrowski, Les points d'attraction et de répulsion pour l'itération dans l'espace à  $n$  dimensions, *C. R. Acad. Sci. Paris* 244 (1957) 288–289.
- [26] A. Ostrowski, *Solution of Equations and Systems of Equations*, Academic Press, New York, 1966.
- [27] J. Ortega, M. Rockoff, Nonlinear difference equations and Gauss–Seidel type iterative methods, *SIAM J. Numer. Anal.* 3 (1966) 497–513.
- [28] J. Kitchen, Concerning the convergence of iterates to fixed points, *Studia Math.* 27 (1966) 247–249.
- [29] W.F. Ames, *Numerical Methods for Partial Differential Equations*, 2nd Edition, Academic Press, New York, 1977.
- [30] C. Huet, Remarques sur l'assimilation d'un matériau hétérogène à un milieu continu équivalent, in: C. Huet, A. Zaoui (Eds.), *Rheological Behaviour and Structure of Materials*, Presses ENPC, Paris, 1981, pp. 231–245.
- [31] C. Huet, Universal conditions for assimilation of a heterogeneous material to an effective medium, *Mech. Res. Commun.* 9 (3) (1982) 165–170.
- [32] C. Huet, On the definition and experimental determination of effective constitutive equations for heterogeneous materials, *Mech. Res. Commun.* 11 (3) (1984) 195–200.
- [33] C. Huet, Application of variational concepts to size effects in elastic heterogeneous bodies, *J. Mech. Phys. Solids.* 38 (1990) 813–841.
- [34] C. Huet, Hierarchies and bounds for size effects in heterogeneous bodies, in: G.A. Maugin (Ed.), *Continuum Models and Discrete Systems*, Vol. 2, 1991, pp. 127–134.
- [36] A. Guidoum, P. Navi, Numerical simulation of thermo-mechanical behaviour of concrete through a 3-D granular cohesive model, in: C. Huet (Ed.), *Micromechanics of Concrete and Cementitious Composites*, Presses Polytechniques et Universitaires Romandes, Lausanne, 1993, pp. 213–228.
- [37] M. Amieur, S. Hazanov, C. Huet, Numerical and experimental study of size and boundary conditions effects on the apparent properties of specimens not having the representative volume, in: C. Huet (Ed.), *Micromechanics of Concrete and Cementitious Composite*, 1993.
- [38] A. Guidoum, Simulation numérique 3D des comportements des btons en tant que composites granulaires, Doctoral Dissertation No. 1310, Ecole Polytechnique de Lausanne, Switzerland, 1994.
- [39] M. Amieur, Etude numérique et expérimentale des effets d'échelle et de conditions aux limites sur des éprouvettes de béton n'ayant pas le volume représentatif, Doctoral Dissertation No. 1256, Ecole Polytechnique Fédérale de Lausanne, Lausanne, Switzerland, 1994.
- [40] S. Hazanov, C. Huet, Order relationships for boundary conditions effect in heterogeneous bodies smaller than the representative volume, *J. Mech. Phys. Solids* 42 (1994) 1995–2011.

- [41] S. Hazanov, M. Amieur, On overall properties of elastic heterogeneous bodies smaller than the representative volume, *Internat. J. Eng. Sci.* 33 (9) (1995) 1289–1301.
- [42] M. Amieur, S. Hazanov, C. Huet, Numerical and experimental assessment of the size and boundary conditions effects for the overall properties of granular composite bodies smaller than the representative volume, in: D.F. Parker, A.H. England (Eds.), *IUTAM Symposium on Anisotropy, Inhomogeneity and Nonlinearity in Solid Mechanics*, Kluwer Academic Publishers, The Netherlands, 1995, pp. 149–154.
- [43] T.I. Zohdi, Computational optimization of vortex manufacturing of advanced materials, *Comput. Meth. Appl. Mech. Eng.* 190 (46–47) (2001) 6231–6256.